ARTICLE

Gold Nanorod Based Selective Identification of *Escherichia coli* Bacteria Using Two-Photon Rayleigh Scattering Spectroscopy

Anant K. Singh, Dulal Senapati, Shuguang Wang, Jelani Griffin, Adria Neely, Perry Candice, Khaleah M. Naylor, Birsen Varisli, Jhansi Rani Kalluri, and Paresh Chandra Ray*

Department of Chemistry, Jackson State University, Jackson, Mississippi 39217

ABSTRACT The presence of *E. coli* in foodstuffs and drinking water is a chronic worldwide problem. The worldwide food production industry is worth about U.S. $578 billion, and the demand for biosensors to detect pathogens and pollutants in foodstuffs is growing day by day. Driven by the need, we report for the first time that two-photon Rayleigh scattering (TPRS) properties of gold nanorods can be used for rapid, highly sensitive and selective detection of *Escherichia coli* bacteria from aqueous solution, without any amplification or enrichment in 50 colony forming units (cfu)/mL level with excellent discrimination against any other bacteria. TPRS intensity increases 40 times when anti-*E. coli* antibody-conjugated nanorods were mixed with various concentrations of *Escherichia coli* O157:H7 bacterium. The mechanism of TPRS intensity change has been discussed. This bionanotechnology assay could be adapted in studies using antibodies specific for various bacterial pathogens for the detection of a wide variety of bacterial pathogens used as bioterrorism agents in food, clinical samples, and environmental samples.

KEYWORDS: gold nanorods · *Escherichia coli* bacteria · two-photon Rayleigh scattering · food pathogens · plasmonics

Escherichia coli (*E. coli*) are members of a large group of bacterial germs that inhabit the intestinal tract of humans and other warm blooded animals. *Escherichia coli* O157:H7 is a human pathogen of animal origin, and as few as 10 cells can cause serious human illness and even death.[1−7] The presence of *E. coli* in foodstuffs and drinking water is a chronic worldwide problem.[1−7] The worldwide food production industry is worth about U.S. $578 billion, and the demand for biosensors to detect pathogens and pollutants in foodstuffs is growing day by day. Conventional methods are selective and sensitive, but since they rely on a series of enrichment steps, they are too slow from the perspective of industrial needs.[1−7] Driven by the need, here we present a nanomaterial-based two-photon Rayleigh scattering assay for sensing of *Escherichia coli* bacteria selectively.

Noble metal nanostructures attract much interest because of their unique properties, including large optical field enhancements resulting in the strong scattering and absorption of light.[8−33] In the last 15 years, the field of biosensors using nanomaterial has witnessed an explosion of interest for small analytes, DNA/RNA, and pathogen detection.[8−33] In terms of sensing, the use of nanotechnology has led to the production of numerous, rapid, sensitive multianalyte assays which are useful not only in the laboratory but also in the field as portable instruments.[8−33] Due to the increased availability of nanostructures with highly controlled optical properties, nanosystems are attractive in their use in technological systems for diagnostic applications. Gold nanosystems attract much interest because of their unique properties, including their shape and size-dependent optical properties. Due to the lack of toxicity,[8−33] scientists have shown great interest in using gold nanosystems for sensing and imaging. The absorption spectra of gold nanorods exhibit two surface plasmon absorption bands, whose origin is localized surface plasmon resonance (LSPR). The longitudinal absorption band is very sensitive to the aspect ratio, and by increasing the aspect ratio (length divided by width), the longitudinal absorption maximum shifts to longer wavelength with an increase in the absorption intensity. Because of the enhanced surface electric field upon surface plasmon excitation, gold nanorods absorb and can scatter electromagnetic radiation strongly. Using the above unique optical property of gold nanorods here, we report for the first time that two-photon Rayleigh scattering (TPRS)

*Address correspondence to paresh.c.ray@jsums.edu.

Received for review March 7, 2009 and accepted June 22, 2009.

Published online July 2, 2009.
10.1021/nn9005494 CCC: $40.75

properties of gold nanorods can be used for rapid, highly sensitive, and selective detection of *Escherichia coli* bacteria from aqueous solution. This nanotechnology method could be adapted for the detection of a wide variety of bacterial pathogens used as bioterrorism agents in food and environmental samples. Our results demonstrate the potential for a broad application of this type of nanotechnology in practical applications in various pathogen detection systems.

RESULTS AND DISCUSSION

Our detection is based on the fact that (1) anti-*E. coli* antibody-conjugated nanorods can readily and specifically identify *Escherichia coli* O157:H7 bacterium, through antibody−antigen recognition (as shown in Figure 1), and (2) when anti-*E. coli* antibody-conjugated nanorods (as shown in Figure 2) were mixed with various concentrations of *Escherichia coli* O157:H7 bacterium, two-photon scattering intensity increases by about 40 times. This increment is due to the fact that *E. coli* bacteria are more than an order of magnitude larger in size (1−3 μm) than the anti-*E. coli* antibody-conjugated gold nanorods. In the presence of *E. coli* bacteria, several gold nanorods conjugate with one *E. coli* bacterium, and as a result, anti-*E. coli* antibody-conjugated gold nanorods undergo aggregation (as shown in Figure 1D). Due to the aggregation, a new broad band appears around 200 nm far from their longitudinal plasmon absorption band, and color change takes place (as shown in Figure 1C). This bioassay is rapid, takes less than 15 min from bacterium binding to detection and analysis, and is convenient and highly selective.

Figure 2A demonstrates how the two-photon scattering intensity varies due to the addition of *E. coli* bacteria to anti-*E. coli* antibody-conjugated gold nanorods. We observed a very distinct two-photon scattering intensity change (4 times) after the addition of 50 cfu/mL *E. coli* bacteria. After the addition of *E. coli* bacteria to anti-*E. coli* antibody-conjugated gold nanorods, the two-photon Rayleigh scattering (TPRS) intensity change observed in our assay can be due to several factors. (1) The intensity of two-photon scattering signal from gold nanorod solution can be expressed as[14−16,20,34−42]

$$I_{TPRS} = G\langle N_w\beta_w^{\,2} + N_{nano}\beta_{nano}^{\,2}\rangle I_\omega^{\,2} e^{-N_{nano}\varepsilon_{2\omega}l} \qquad (1)$$

where G is a geometric factor, N_w and N_{nano} are the number of water molecules and gold nanorods per unit volume, β_w and β_{nano} are the quadratic hyperpolarizabilities of a single water molecule and a single gold nanoparticle, $\varepsilon_{2\omega}$ is the molar extinction coefficient of the gold nanoparticle at 2ω, l is the path length, and I_ω is the fundamental intensity. The exponential factor accounts for the losses through absorption at the harmonic frequency. Since there is a center of inversion in the nanorod, the TPRS intensity arising from gold nanorods cannot be due to electric dipole contribution. Considering the size of a nanorod, the approximation that assumes that the electromagnetic fields are spatially constant over the volume of the particle may not suitable anymore. As a result, the total nonlinear polarization consists of different contributions such as multipolar radiation of the harmonic energy of the excited dipole and possibly of higher multipoles, as we discussed in our previous publication or reported by others.[14−16,20,34−42] The HRS intensity therefore also consists of several contributions. The first one is the electric dipole approximation, which may arise due to the defects in the nanoparticle. This contribution is actually identical to the one observed for any noncentrosymmetrical point-like objects such as efficient rod-like push−pull molecules. The second contribution is multipolar contribution like electric quadrupole contribution. This contribution is very important when the size of the particle is no longer negligible when compared to the wavelength, as we reported before. Since *E. coli* bacteria are more than an order of magnitude larger in size (1−3 μm) than the anti-*E. coli* antibody-conjugated gold nanorods, several gold nanorods conjugate to one *E. coli* bacterium, and as a result, anti-*E. coli* antibody-conjugated gold nanorods undergo aggregation in the presence of *E. coli* bacteria (as shown in Figure 2C−F). Due to the aggregation in the presence of *E. coli* bacteria, nanorods lose the center of symmetry, and as a result, one can expect a significant amount of electric dipole contribution to the two-photon scattering intensity. Since electric dipole contributes several times higher than that of multipolar moments, we expect two-photon scattering intensity to increase with aggregation. (2) When *E. coli* bacteria are added to the anti-*E. coli* antibody-conjugated gold nanorods, a clear colorimetric change is observed due

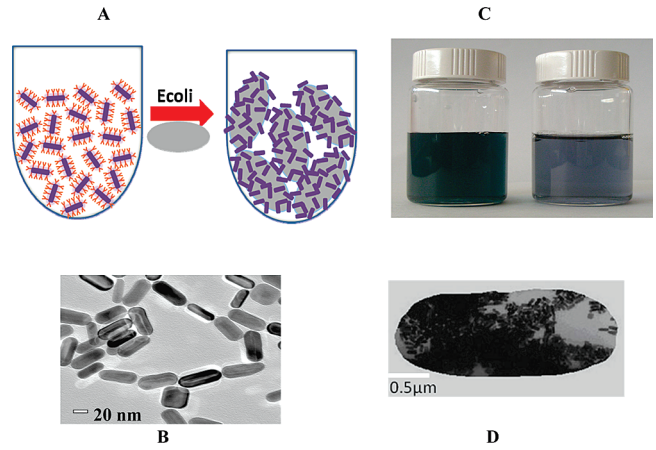

Figure 1. (A) Schematic representation of anti-*E. coli* antibody-conjugated nanorod-based sensing of *E. coli* bacteria. (B) TEM image of anti-*E. coli* antibody-conjugated nanorods before addition of *E. coli* bacteria. (C) Photograph showing colorimetric change upon addition of *E. coli* bacteria (10^4 cfu/mL), and (D) TEM image demonstrating aggregation of gold nanorods after the addition of *E. coli* bacteria (10^3 cfu/mL).

to the aggregation. As shown in Figure 2B, absorption maximum for the longitudinal absorption band at 680 nm decreases with the increase of the concentration of *E. coli* bacteria, whereas a new broad band corresponding to the absorption of nanorod aggregates at 950 nm increases with the increment of the concentration of *E. coli* bacteria. According to the two-state model[43]

$$\beta^{\text{two state}} = \underbrace{\frac{3\mu_{eg}^{2}\Delta\mu_{eg}}{E_{eg}^{2}}}_{\text{static factor}} \quad \underbrace{\frac{\omega_{eg}^{4}}{(\omega_{eg}^{2} - 4\omega^{2})(\omega_{eg}^{2} - \omega^{2})}}_{\text{dispersion factor}} \tag{2}$$

where ω is the fundamental energy of the incident light, μ_{eg} is the transition dipole moment, and ω_{eg} is the transition energy between the ground state $|g\rangle$ and the charge-transfer excited state $|e\rangle$, $\Delta\mu_{eg}$ is the difference in dipole moment between $|e\rangle$ and $|g\rangle$ states.

Since $\omega_{eg} \propto 1/\lambda_{max}$, and λ_{max} shifted 270 nm toward red upon addition of bacteria (as shown in Figure 2B), β should change tremendously upon the addition of bacteria, and as a result, the two-photon scattering intensity should change tremendously with the addition of *E. coli* bacteria. (3) The single photon resonance enhancement and two-photon luminescence factors are much larger for nanorod aggregates due to the closeness of λ_{max} to the fundamental wavelength at 860 nm. This factor should increase two-photon scattering intensity. (4) Since size increases tremendously with aggregation, the two-photon scattering intensity should increase with the increase in particle size. (5) The aggregation of gold nanorods can enhance the scattering intensity because the local electric field enhancement becomes larger owing to the surface plasmon resonance coupling.

We also noted that, though two-photon scattering intensity changes about 4 times even at the concentration of 50 cfu/mL of *E. coli* bacteria, the visible color changes can be observed only after the addition of 10 000 cfu/mL bacteria, which indicates that our two-photon scattering-based gold nanorod assay is about 2 orders of magnitude more sensitive than the usual colorimetric technique.

To understand whether our assay is highly selective, we have also performed how two-photon scattering intensity changes upon addition of *Salmonella typhimurium* bacteria to anti-*E. coli* antibody-conjugated gold nanorods. As shown in Figure 2A, two-photon scattering intensity changes only 6% when we added the *Salmonella typhimurium* bacteria to anti-*E. coli* antibody-conjugated gold nanorods. Similarly, when we added *E. coli* bacteria to anti-*Salmonella* antibody-conjugated gold nanorods, two-photon scattering intensity changes only 5%. So the above data demonstrate that our assay is highly selective.

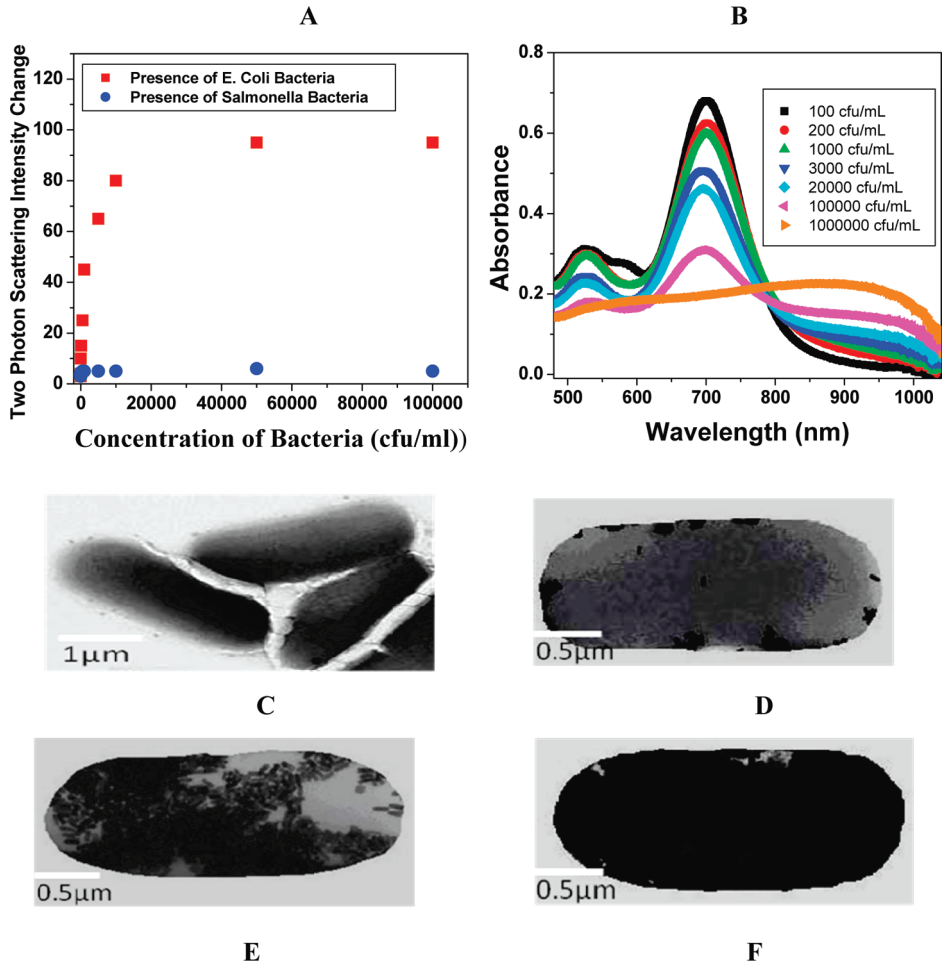

Figure 2. (A) Plot demonstrating two-photon scattering intensity changes (by 40 times) due to the addition of *E. coli* bacteria to anti-*E. coli* antibody-conjugated gold nanorods. Two-photon scattering intensity changes very little upon addition of *Salmonella* bacteria. (B) Absorption profile variation of anti-*E. coli* antibody-conjugated Au nanorods due to the addition of different concentrations of *E. coli* bacteria (10^2 to 10^7 cfu/mL). The strong long wavelength band in the near-infrared region (λ_{LPR} = 680 nm) is due to the longitudinal oscillation of the conduction band electrons. The short wavelength peak ($\lambda \approx 520$ nm) is from the nanorods' transverse plasmon mode. New band appearing around 950 nm, due to the addition of *E. coli* bacteria, demonstrates the aggregation of gold nanorods. (C) TEM image of *E. coli* bacteria before addition of nanorod. (D) TEM image after addition of 10^2 cfu/mL *E. coli* bacteria. (E) TEM image demonstrating aggregation of gold nanorods after the addition of 8×10^4 cfu/mL *E. coli* bacteria. (F) TEM image demonstrating aggregation of gold nanorods after the addition of 10^7 cfu/mL *E. coli* bacteria.

To evaluate whether our assay is selective to O157:H7 in the presence of other *E. coli* strains, we have also measured two-photon scattering intensity changes upon addition of different *E. coli* strains O157:H7, O157:NM, and O157:non-H7 separately. As shown in Figure 3, two-photon scattering intensity changes only 1.7−2.4 times when we added O157:NM and O157:non-H7 strains to monoclonal antibody (MAbs 2B7)-coated gold nanorod colloidal solution. So our results shows that our assay is quite selective over other *E. coli* strains.

Our results also indicate that (as shown in Figure 2A), the TPRS intensity changes linearly with the concentration of the *E. coli* bacteria at the lower concentration range. To evaluate whether our assay is capable of measuring *E. coli* bacteria concentration quantitatively, we performed two-photon Rayleigh scattering intensity measurements at different concentrations of target *E. coli* bacteria at lower concentration range. As shown in Figure 4, the two-photon scattering intensity increment is highly sensitive to the concentration of target *E. coli* bacteria over the range of 50−2100 cfu/mL, and the intensity increased linearly with concentration. Our data indicate that our assay exhibits a detection limit to detect *E. coli* bacteria as low as 50 cfu/mL. So our gold nanorod-based two-photon scattering assay can provide a quantitative measurement of *E. coli* bacteria concentration over 50−2100 cfu/mL concentration range.

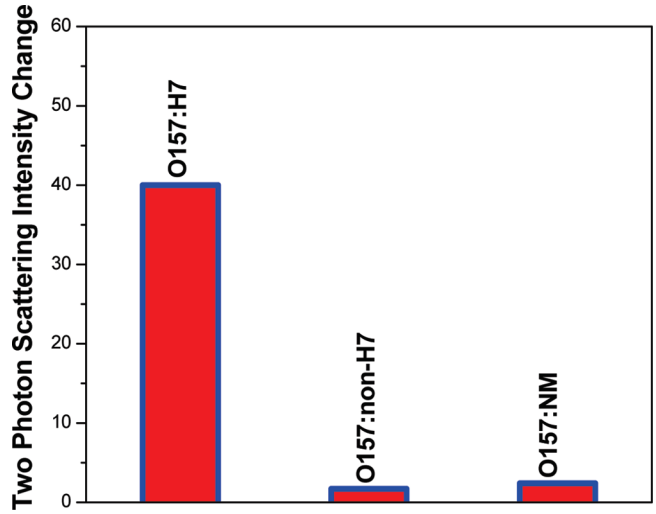

Figure 3. Plot demonstrating selectivity of our two-photon scattering assay over different *E. coli* strains. Two-photon scattering intensity changes 40 times due to the addiction of *E. coli* O157:H7 strains to specific anti-*E. coli* antibody (MAbs 2B7)-conjugated gold nanorods. Two-photon scattering intensity changes only 1.7−2.4 times upon addition of O157:NM and O157:non-H7 strains.

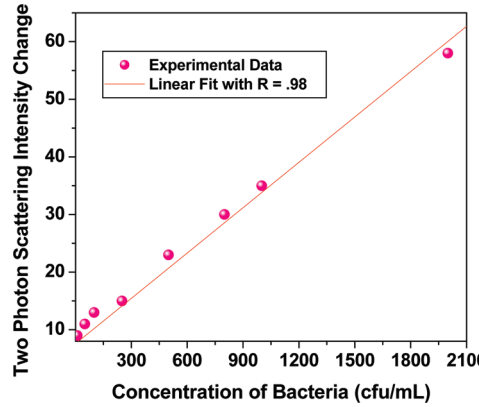

Figure 4. Plot demonstrating linear correlation between two-photon scattering intensity and concentration of *E. coli* bacteria over the range of 50−2100 cfu/mL with $R = 0.985$.

CONCLUSIONS

In conclusion, in this paper, we have demonstrated for the first time a fast and highly sensitive assay for *E. coli* bacteria detection using antibody-conjugated gold nanorod-based two-photon scattering technique. We have shown that when anti-*E. coli* antibody-conjugated nanorods were mixed with various concentrations of *Escherichia coli* O157:H7 bacteria, two-photon scattering intensity increases by about 40 times. Our experiment indicates that *E. coli* bacteria can be detected quickly and accurately without any amplification or enrichment in 50 cfu/mL level with excellent discrimination against any other bacteria. This bioassay is rapid and takes less than 15 min from bacteria binding to detection and analysis. Our experimental study clearly shows that this nanorod-based assay is highly selective. Our results point out that our antibody-conjugated gold nanorod-based two-photon scattering assay can provide a quantitative measurement of *E. coli* bacteria concentration. Our experimental results reported here open up a new possibility of rapid, easy, and reliable diagnosis of food pathogens by measuring the TPRS intensity from bacteria-modified gold nanorods. The examples of the applications of noble metal nanostructures provided herein can be readily generalized to other areas of biology and medicine because plasmonic nanomaterials exhibit great range, versatility, and systematic tunability of their optical attributes. It is probably possible to improve the sensitivity of our two-photon scattering assay by several orders of magnitude by choosing proper nanomaterials and detection systems. Looking into the future, we expect that these sensor developments will have important implications in the development of better biosensors and bioassay for application to clinical analysis and biomedical research.

EXPERIMENTAL METHODS

Hydrogen tetrachloroaurate ($HAuCl_4 \cdot 3H_2O$), $NaBH_4$, silver nitrate, cetyltrimethylammonium bromide (CTAB), glutaraldehyde, buffer solution, sodium chloride, and sodium citrate were purchased from Sigma-Aldrich and used without further purification. Anti-*E. coli* antibodies were purchased from Biodesign International.

Synthesis and Characterization of Anti-*E. coli* Antibody-Conjugated Gold Nanorods. Gold nanorods were synthesized using a seed-mediated, surfactant-assisted growth method in a two-step

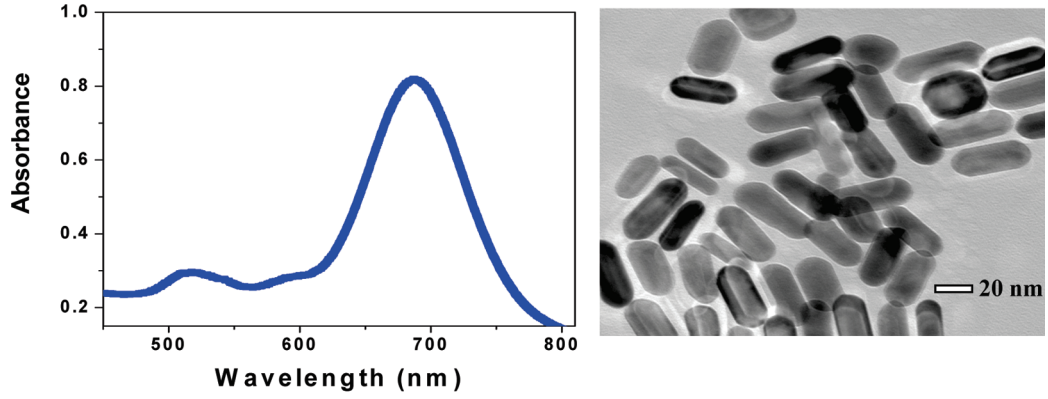

Figure 5. (A) Extinction profile of Au nanorods with aspect ratios from 2.7. The strong, long wavelength band in the near-infrared region (λ_{LPR} = 680 nm) is due to the longitudinal oscillation of the conduction band electrons. The short wavelength peak ($\lambda \approx$ 520 nm) is from the nanorods' transverse plasmon mode. (B) TEM image of nanorods of average aspect ratios (σ) ≈ 2.7.

procedure.[20−25] Nanorods were purified by several cycles of suspension in ultrapure water, followed by centrifugation. Nanorods were isolated in the precipitate, and excess CTAB was removed in the supernatant. Nanorods were characterized by TEM and absorption spectroscopy (as shown in Figure 5A,B).

The nanorods prepared by the above methods were capped with a bilayer of cetyltrimethylammonium bromide (CTAB), which is positively charged. For the preparation of anti-*E. coli* antibody-conjugated nanorods, we modified the gold nanorod surface by amine groups (as shown in Scheme 1) using cystamine dihydrochloride and a reported method.[25] For this purpose, we have added 30 mM cystamine dihydrochloride to a gold nanorod, and the solution was kept at 60 °C for several hours under constant sonication. Excess cystamine dihydrochloride was removed by centrifugation at 8000 rpm for several minutes.

For covalent immobilization of the antibody onto the amine-modified gold nanorod surface, we have used a highly established glutaraldehyde spacer method. In brief, 10 mL of amine-functionilized nanorods was incubated with anti-*E. coli* antibody for 18 h at 4 °C in PBS media. After that, we washed the anti-*E. coli* antibody-conjugated gold nanorod several times with PBS to remove excess antibody. We have not noted any aggregation of gold nanorod during amine group activation and immobilization of the antibody.

Bacteria Sample Preparation and Bacteria Nanomaterial Interaction. Bacteria samples were collected after the bacteria were cultured for 16 h. Phosphate buffered saline (PBS) was added to the sample, and the sample was vortexed and then centrifuged. After that, different concentrations (in cfu/mL) of bacteria were added to anti-*E. coli* antibody-conjugated gold nanorod solutions for 30−45 min. After half an hour, one drop of mixture sample was placed on a mesh for TEM experiment. TEM experiment was performed using JEM-2100F advanced field emission electron microscope, operating at 100−200 kV.

Two-Photon Scattering Experiment Details. Two-photon scattering properties have been monitored using hyper-Rayleigh scattering (HRS) technique.[14−16,20,34−42] The intensity of the single photon light scattering or Rayleigh scattering is linearly dependent on the number density and the impinging laser intensity and quadratically on the linear polarizability α. The two-photon light scattering or hyper-Rayleigh scattering can be observed from fluctuations in symmetry, caused by rotational fluctuations. This is a second harmonic generation experiment in which the light is scattered in all directions rather than as a narrow coherent beam. For the HRS experiment, we have used a mode-locked Ti:sapphire laser delivering at the fundamental wavelength of 860 nm with a pulse duration of about 150 fs at a repetition rate of 80 MHz. We performed TEM data analysis before and after exposure of about 5 min to the laser, and we have not noted any photothermal damage of gold nanorods within our HRS data collecting time. The HRS light was separated from its linear counterpart by a high-pass filter and a monochromator and then detected with a cooled photomultiplier tube, and the pulses were counted with a photon counter. The fundamental input beam was linearly polarized, and the input angle of polarization was selected with a rotating half-wave plate. In all experiments reported, the polarization state of the harmonic light was vertical. Since nanorods are known[9,22] to possess strong two-photon luminescence (TPL), to avoid TPL contributions from the HRS signal, we have used the following steps: (1) We have used gold nanorods of aspect ratio 2.7, whose λ_{max} is about 200 nm far from the excitation wavelength. (2) We have used 430 nm interference filter with 3 nm bandwidth in front of PMT to make sure that only a second harmonic signal is collected by PMT. To understand whether the two-photon scattering intensity at 430 nm light is due to second harmonic generation, we performed power-dependent as well as concentration-dependent studies. Figure 6 shows the output signal intensities at 430 nm from anti-*E. coli* antibody-conjugated gold nanorods at different powers of 860 nm incident light. A linear nature of the plot implies that the doubled light is indeed due to the two-photon Rayleigh scattering signal.

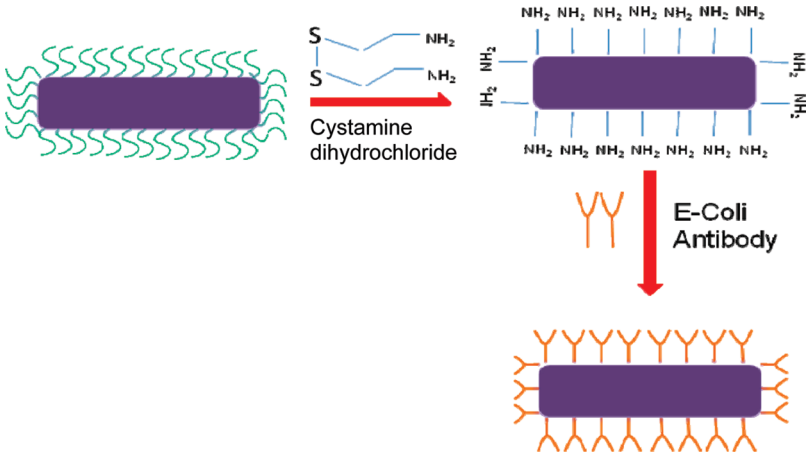

Scheme 1. Schematic representation of the synthesis of anti-*E. coli* antibody-conjugated nanorod.

Acknowledgment. P.C.R. thanks NIH-SCORE Grant No. S06GM 008047, NSF-PREM Grant No. DMR-

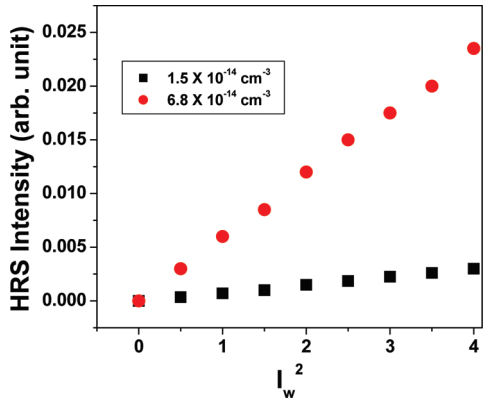

Figure 6. Power dependence of scattering intensity at different concentrations of *E. coli* antibody-conjugated gold nanorods.

0611539, and NSF-CREST Grant No. HRD-0833178 for their generous funding. We thank Sara H. Bayley, Instrumentation Facilities Coordinator, University of Southern Mississippi, for helping to acquire TEM data. We also thank reviewers whose valuable suggestions improved the quality of the manuscript.

REFERENCES AND NOTES

1. Armstrong, G. L.; Hollingsworth, J.; Morris, J. G., Jr. Emerging Foodborne Pathogens: *Escherichia coli* O157:H7 as a Model of Entry of a New Pathogen into the Food Supply of the Developed World. *Epidemiol. Rev.* **1996**, *18*, 29–51.
2. Li, J.; Hovde, C. J. Expression Profiles of Bovine Genes in the Rectoanal Junction Mucosa during Colonization with *Escherichia coli* O157:H7. *Appl. Environ. Microbiol.* **2007**, *73*, 2380–2385.
3. Phillips, C. A. The Epidemiology, Detection and Control of *Escherichia coli* O157. *J. Sci. Food Agric.* **1999**, *79*, 1367–1381.
4. Ram, S.; Vajpayee, P.; Shanker, R. Rapid Culture-Independent Quantitative Detection of Enterotoxigenic *Escherichia coli* in Surface Waters by Real-Time PCR with Molecular Beacon. *Environ. Sci. Technol.* **2008**, *42*, 4577–4582.
5. ERS, http://ers.usda.gov/Briefing/FoodborneDisease.
6. Butler, D. Novel Pathogens Beat Food Safety Checks. *Nature* **1996**, *384*, 397.
7. Xue, C.; Velayudham, S.; Johnson, S.; Saha, R.; Smith, A.; Brewer, W.; Murthy, P.; Bagley, S. T.; Liu, H. Highly Water-Soluble, Fluorescent, Conjugated Fluorene-Based Glycopolymers with Poly(ethylene glycol)-Tethered Spacers for Sensitive Detection of *Escherichia coli*. *Chem.—Eur. J.* **2009**, *15*, 2289.
8. Stewart, M. E.; Anderton, C. R.; Thompson, L. B.; Maria, J.; Gray, S. K.; Rogers, J. A.; Nuzzo, R. G. Nanostructured Plasmonic Sensors. *Chem. Rev.* **2008**, *108*, 494–521.
9. Durr, N. J.; Larson, T.; Smith, D. K.; Korgel, B. A.; Sokolov, K.; Yakar, A. B. Two-Photon Luminescence Imaging of Cancer Cells Using Molecularly Targeted Gold Nanorods. *Nano Lett.* **2007**, *7*, 941–945.
10. Ni, W.; Yang, Z.; Chen, H.; Li, L.; Wang, J. Coupling between Molecular and Plasmonic Resonances in Freestanding Dye−Gold Nanorod Hybrid Nanostructures. *J. Am. Chem. Soc.* **2008**, *130*, 6692–6693.
11. Kell, A. J.; Stewart, G.; Ryan, S.; Peytavi, R.; Boissinot, B.; Huletsky, A.; Bergeron, M. G.; Simard, B. Vancomycin-Modified Nanoparticles for Efficient Targeting and Preconcentration of Gram-Positive and Gram-Negative Bacteria. *ACS Nano* **2008**, *2*, 1777–1788.
12. Darbha, G. K.; Ray, A.; Ray, P. C. Gold-Nanoparticle-Based Miniaturized FRET Probe for Rapid and Ultra-Sensitive Detection of Mercury in Soil, Water and Fish. *ACS Nano* **2007**, *1*, 208–214.
13. Griffin, J.; Singh, A. K.; Senapati, D.; Rhodes, P.; Mitchell, K.; Robinson, B.; Yu, E.; Ray, P. C. Size and Distance Dependent NSET Ruler for Selective Sensing of Hepatitis C Virus RNA. *Chem.—Eur. J.* **2009**, *15*, 342–351.
14. Griffin, J.; Singh, A. K.; Senapati, D.; Lee, E.; Gaylor, K.; Jones-Boone, J.; Ray, P. C. Sequence Specific HCV-RNA Quantification Using Size Dependent Nonlinear Optical Properties of Gold Nanoparticles. *Small* **2009**, *5*, 839–845.
15. Darbha, G. K.; Singh, A. K.; Rai, U. S.; Yu, E.; Yu, H.; Ray, P. C. Highly Selective Detection of Hg^{2+} Ion Using NLO Properties of Gold Nanomaterial. *J. Am. Chem. Soc.* **2008**, *130*, 8038.
16. Ray, P. C. Label-Free Diagnostics of Single Base-Mismatch DNA Hybridization on Gold Nanoparticles Using Hyper-Rayleigh Scattering Technique. *Angew. Chem., Int. Ed* **2006**, *45*, 1151–1154.
17. Ni, W.; Kou, X.; Yang, Z.; Wang, J. Tailoring Longitudinal Surface Plasmon Wavelengths, Scattering and Absorption Cross-Sections of Gold Nanorods. *ACS Nano* **2008**, *2*, 677–686.
18. Mayer, K. M.; Lee, S.; Liao, H.; Rostro, B. C.; Fuentes, A.; Scully, P. T.; Nehl, C. L.; Hafner, J. H. A Label-Free Immunoassay Based Upon Localized Surface Plasmon Resonance of Gold Nanorods. *ACS Nano* **2008**, *2*, 687–692.
19. Wijaya, A.; Schaffer, S. B.; Pallares, I. G.; Kimberly, H.-S. Selective Release of Multiple DNA Oligonucleotides from Gold Nanorods. *ACS Nano* **2009**, *3*, 80–86.
20. Darbha, G. K.; Rai, U. S.; Singh, A. K.; Ray, P. C. Gold Nanorod Based Sensing of Sequence Specific HIV-1 Virus DNA Using Hyper Rayleigh Scattering Spectroscopy. *Chem.—Eur. J.* **2008**, *14*, 3896–3903.
21. Liao, H.; Hafner, J. H. Gold Nanorod Bioconjugates. *Chem. Mater.* **2005**, *17*, 4636–4641.
22. Huang, X.; El-Sayed, I. H.; Qian, W.; El-Sayed, M. A. Cancer Cell Imaging and Photothermal Therapy in the Near-Infrared Region by Using Gold Nanorods. *J. Am. Chem. Soc.* **2006**, *128*, 2115–2120.
23. Berry, V.; Gole, A.; Kundu, S.; Murphy, C. J.; Saraf, R. F. Deposition of CTAB-Terminated Nanorods on Bacteria to Form Highly Conducting Hybrid Systems. *J. Am. Chem. Soc.* **2005**, *127*, 17600.
24. Murphy, C. J.; Sau, T. K.; Gole, A. M.; Orendroff, C. J.; Gao, J.; Gou, L.; Hunyadi, S. E.; Li, T. Anisotropic Metal Nanoparticles: Synthesis, Assembly, and Optical Applications. *J. Phys. Chem. B* **2005**, *109*, 13857–13870.
25. Wang, C.; Irudayaraj, J. Gold Nanorod Probe for the Detection of Multiple Pathogens. *Small* **2008**, *4*, 2004.
26. Pietrobon, B.; McEachran, M.; Kitaev, V. Synthesis of Size-Controlled Faceted Pentagonal Silver Nanorods with Tunable Plasmonic Properties and Self-Assembly of These Nanorods. *ACS Nano* **2009**, *3*, 21–26.
27. Chen, Y.; Munteanu, C. A.; Huang, Y.-F.; Phillips, J.; Zhu, Z.; Mavros, M.; Tan, W. Mapping Receptor Density on Live Cells by Using Fluorescence Correlation Spectroscopy. *Chem.—Eur. J.* **2009**, *21*, 5327–5336.
28. Tang, B.; Cao, L.; Xu, K.; Zhuo, L.; Ge, J.; Li, Q.; Yu, L. A New Nanobiosensor for Glucose with High Sensitivity and Selectivity in Serum Based on Fluorescence Resonance Energy Transfer (FRET) between CdTe Quantum Dots and Au Nanoparticles. *Chem.—Eur. J.* **2008**, *14*, 3637.
29. Satyabrata, S.; Mandal, T. K. Tryptophan-Based Peptides to Synthesize Gold and Silver Nanoparticles: A Mechanistic and Kinetic Study. *Chem.—Eur. J.* **2007**, *27*, 3160–3168.
30. Alivisatos, P. The Use of Nanocrystals in Biological Detection. *Nat. Biotechnol.* **2004**, *22*, 47–52.
31. Xiang, J.; Lu, W.; Hu, Y.; Wu, Y.; Yan, H.; Lieber, C. M. High Performance Field Effect Transistors Based on Ge/Si Nanowire Heterostructures. *Nature* **2006**, *441*, 489.
32. Cao, Y. W. C.; Jin, R. C; Mirkin, C. A. Nanoparticles with Raman Spectroscopic Fingerprints for DNA and RNA Detection. *Science* **2002**, *297*, 1536–1540.
33. Donath, E. Biosensors: Viruses for Ultrasensitive Assays. *Nat. Nanotechnol.* **2009**, *4*, 215–216.

34. Duncan, V.; Song, K.; Hung, S.-T.; Miloradovic, I.; Nayak, A.; Persoons, A.; Verbiest, T.; Therien, M. J.; Clays, K. Molecular Symmetry and Solution-Phase Structure Interrogated by Hyper-Rayleigh Depolarization Measurements: Elaborating Highly Hyperpolarizable. *Angew. Chem., Int. Ed.* **2008**, *47*, 2978–2981.
35. Sporer, C.; Ratera, I.; Zho, Y.; Gancedo, J. V.; Wurst, K.; Jaitner, P.; Clays, K.; Persoons, A.; Rovira, C.; Veciana, J. A. Molecular Multiproperty Switching Array Based on the Redox Behavior of a Ferrocenyl Polychlorotriphenylmethyl Radical. *Angew. Chem., Int. Ed* **2004**, *43*, 5266.
36. Murillo, M. T.; Prados, P.; Al-Saraierh, H.; El-Dali, A.; Thompson, D. W.; Collins, J.; Georghiou, P. E.; Teshome, A.; Asselberghs, I.; Clays, K. Alkynyl Expanded Donor−Acceptor Calixarenes: Geometry and Second-Order Nonlinear Optical Properties. *Chem.—Eur. J.* **2007**, *27*, 7753–7761.
37. Antione, I.-R.; Jonin, C.; Nappa, J.; Benichou, E.; Brevet, P. F. Wavelength Dependence of the Hyper-Rayleigh Scattering Response from Gold Nanoparticles. *Chem. Phys.* **2004**, *120*, 10748.
38. Chandra, M.; Indi, S. S.; Das, P. K. Depolarized Hyper-Rayleigh Scattering from Copper Nanoparticles. *J. Phys. Chem. C* **2007**, *111*, 10652.
39. Russier-Antoine, I.; Benichou, E.; Bachelier, G.; Jonin, C.; Brevet, P. F. Multipolar Contributions of the Second Harmonic Generation from Silver and Gold Nanoparticles. *J. Phys. Chem. C* **2007**, *111*, 9044–9048.
40. Clays, K.; Persoons, A. Hyper-Rayleigh Scattering in Solution. *Phys. Rev. Lett.* **1991**, *66*, 2980–2983.
41. Dadap, J. I.; Shan, J.; Eisenthal, K.; Heinz, T. F. Second-Harmonic Rayleigh Scattering From a Sphere of Centrosymmetric Materials. *Phys. Rev. Lett.* **1999**, *83*, 4045.
42. Novak, J. P.; Brousseau, L. C.; Vance, F. W.; Johnson, R. C.; Lemon, B. I.; Hupp, J. T.; Feldheim, D. L. Assembly of Phenylacetylene-Bridged Gold and Silver Nanoparticle Arrays. *J. Am. Chem. Soc.* **2000**, *122*, 12029–12030.
43. Oudar, J. L. Optical Nonlinearities of Conjugated Molecules. Stilbene Derivatives and Highly Polar Aromatic Compounds. *J. Chem. Phys.* **1977**, *67*, 446–457.